

Formulation of the Relativistic Quantum Hall Effect and “Parity Anomaly”

Kouki Yonaga¹, Kazuki Hasebe², and Naokazu Shibata¹

¹*Department of Physics, Tohoku University, Sendai, 980-8578, Japan*

²*National Institute of Technology, Kagawa College, Mitoyo, Kagawa, 769-1103, Japan*

(Dated: December 9, 2024)

We present a relativistic formulation of the quantum Hall effect on a Riemann sphere. An explicit form of the pseudopotential is derived for the relativistic quantum Hall effect with/without mass term. We clarify particular features of the relativistic quantum Hall states with use of the exact diagonalization study of the pseudopotential Hamiltonian. Physical effects of the mass term to relativistic quantum Hall states are investigated in detail. The mass term acts as an interpolating parameter between the relativistic and non-relativistic quantum Hall effects. It is pointed out that the mass term inequivalently affects to many-body physics of the positive and negative Landau levels and brings instability of the Laughlin state of the positive first relativistic Landau level as a consequence of the “parity anomaly”.

I. INTRODUCTION

Dirac matter has attracted considerable attention in condensed matter physics for its novel properties and recent experimental realizations in solid materials. In contrast to normal single-particle excitations in solids, Dirac particles exhibit linear dispersion in a low energy region and continuously vanishing density of states at the charge-neutral point [1]. These features are actually realized in graphene [2, 3] and on topological insulator surface [4]. Besides, when magnetic field is applied to them, the relativistic quantum Hall effects were observed in graphene [5–7] and also on topological insulator surface recently [8, 9].

One of the most intriguing features of the relativistic quantum Hall effect is the effect of mass term: In the non-relativistic quantum Hall effect the mass parameter just tunes the Landau level spacing, while in the relativistic quantum Hall effect the mass term is concerned with interesting physics such as semi-metal to insulator transition and time reversal symmetry breaking of the topological insulator [10]. In experiments, disorder and interaction with a substrate in the atomic layer of graphene make asymmetry in the two sublattice of honeycomb structure to induce mass term [11, 12] and magnetic doping in topological insulator yields a massive gap of the surface Dirac cone [13]. Interestingly in the presence of the external magnetic field, the mass term brings physics associated with the “parity anomaly” [14]: In the absence of the magnetic field, the mass term does not change the equivalence between the positive and negative energy levels [15], while in the presence, asymmetry occurs between the positive and negative energy levels depending on the sign of the mass parameter [16] [see Fig.1].

In this paper we establish a relativistic formulation of the quantum Hall effect on a Riemann sphere and perform a first investigation of the “parity anomaly” in the context of the relativistic *many-body* physics. For concrete calculations, the spherical geometry called Hal-

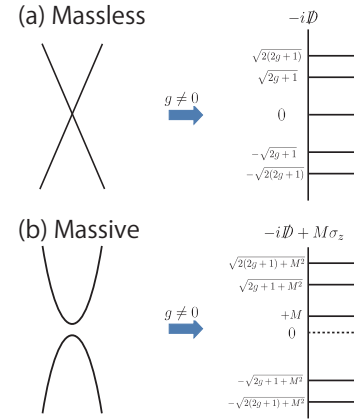


FIG. 1. (Color online) Schematic of the energy spectrum and Landau level. (a) and (b) show the massless and the massive case ($M > 0$), respectively. (g represents a monopole charge.) The right figure of (b) shows asymmetry between the positive and negative energy levels due to the absence of $-M$. (In general, there exists the energy level $E = +\text{sgn}(g \cdot M) |M|$ while not $E = -\text{sgn}(g \cdot M) |M|$.) The original reflection symmetry of the energy levels with respect to the zero-energy is broken due to the mass term.

dane sphere [17] is adopted. Instead of using approximate pseudopotential of the infinite disk geometry in the previous study [18], we construct an *exact* form of the pseudopotential based on the relativistic Landau model recently analyzed by one of the authors [19]. Previous numerical studies on fractional quantum Hall states in graphene show the existence of Laughlin state at $\nu = 1/3$ even in $n = 1$ Landau level [20, 21] where the charge excitation gap is larger than that of $n = 0$ Landau level. This stability of Laughlin state in $n = 1$ Landau level is a unique feature of the linear dispersion of Dirac equation. We study how this stability of Laughlin states changes with increase of mass. Based on the exact diagonalization we numerically obtain a many-body ground state of the relativistic pseudopotential Hamiltonian, and analyze the mass effect to the Laughlin state at $\nu = \frac{1}{3}$ in

the $n = 1$ relativistic Landau level.

II. RELATIVISTIC LANDAU PROBLEM ON A SPHERE

In this section, we give a brief review of the relativistic Landau problem on the Haldane's sphere [19] and discuss its mass deformation. The monopole gauge field is given by [22, 23]

$$A = -g \cos \theta d\phi, \quad (2.1)$$

where g denotes the monopole charge. (In the following, we assume that g is positive for simplicity.) The Dirac operator on a two-sphere in the monopole background can be represented as

$$\begin{aligned} -i\mathcal{D} &= -i\frac{1}{R_s}\sigma_x\partial_\theta - i\frac{1}{R_s\sin\theta}\sigma_y(\partial_\phi + i(g - \frac{1}{2}\sigma_z)\cos\theta) \\ &= -i\frac{1}{R_s}\sigma_x(\partial_\theta + \frac{1}{2}\cot\theta) - i\sigma_y\frac{1}{R_s\sin\theta}(\partial_\phi + ig\cos\theta), \end{aligned} \quad (2.2)$$

or

$$-i\mathcal{D} = \frac{1}{R_s} \begin{pmatrix} 0 & -i\mathfrak{D}_-^{(g+\frac{1}{2})} \\ -i\mathfrak{D}_+^{(g-\frac{1}{2})} & 0 \end{pmatrix}. \quad (2.3)$$

Here R_s is the radius of the Haldane sphere and $\mathfrak{D}_\pm^{(g+\frac{1}{2})}$ are the edth operators [24]:

$$\mathfrak{D}_\pm^{(g)} = \partial_\theta \mp ig \cot \theta \pm i\frac{1}{\sin\theta}\partial_\phi. \quad (2.4)$$

For graphene, two components of the Dirac spinor indicate sublattice degrees of freedom, while for topological insulator the real spin degrees of freedom of surface electron. The eigenvalues of the Dirac operator (2.2) are derived as

$$\pm \lambda_n = \pm \frac{1}{R_s} \sqrt{n(n+2g)}, \quad (n = 0, 1, 2, \dots) \quad (2.5)$$

where n corresponds to the relativistic Landau level index. Notice that the spectrum (2.5) exhibits the reflection symmetry with respect to the zero energy. Each Landau level $\pm \lambda_n$ exhibits the following degeneracy

$$d_{\lambda_n} = d_{-\lambda_n} = 2(g+n). \quad (2.6)$$

The degenerate eigenstates of the Landau level are

$$n = 1, 2, \dots:$$

$$\psi_{\pm\lambda_n, m}^g(\theta, \phi) = \frac{1}{\sqrt{2}} \begin{pmatrix} Y_{j=(g-\frac{1}{2})+n, m}^{g-\frac{1}{2}}(\theta, \phi) \\ \mp i Y_{j=(g+\frac{1}{2})+(n-1), m}^{g+\frac{1}{2}}(\theta, \phi) \end{pmatrix}, \quad (2.7a)$$

$$n = 0 : \psi_{\lambda_0=0, m}^g(\theta, \phi) = \begin{pmatrix} Y_{j=(g-\frac{1}{2}), m}^{g-\frac{1}{2}}(\theta, \phi) \\ 0 \end{pmatrix}, \quad (2.7b)$$

with $m = -g + \frac{1}{2} + n, -g + \frac{3}{2} + n, \dots, g - \frac{1}{2} + n$. $Y_{j, m}^g$ denote the monopole harmonics [22]:

$$\begin{aligned} Y_{l, m}^g(\theta, \phi) &= 2^m \sqrt{\frac{(2l+1)(l-m)!(l+m)!}{4\pi(l-g)!(l+g)!}} \\ &\times (1-x)^{-\frac{m+g}{2}}(1+x)^{-\frac{m-g}{2}} P_{l+m}^{(-m-g, -m+g)}(x) \cdot e^{im\phi}, \end{aligned} \quad (2.8)$$

where $x = \cos \theta$ and $P_n^{(\alpha, \beta)}(x)$ stands for the Jacobi polynomials.

Notice that the components of $\psi_{\pm\lambda_n, m}^g$ (2.7a) consist of the monopole harmonics in different non-relativistic Landau levels, n and $n-1$, and carry the same $SU(2)$ index

$$j = g - \frac{1}{2} + n, \quad (2.9)$$

which implies that $\psi_{\pm\lambda_n, m}^g$ itself transforms as the $SU(2)$ irreducible representation. Such $SU(2)$ angular momentum operators are given by

$$J_i = -i\epsilon_{ijk}x_j(\partial_k - i\mathcal{A}_k) - (g - \frac{1}{2}\sigma_z)\frac{x_i}{r}, \quad (2.10)$$

with

$$\mathcal{A} = \mathcal{A}_i dx_i = -(g - \frac{1}{2}\sigma_z) \cos \theta d\phi. \quad (2.11)$$

Notice that J_i (2.10) is simply obtained as the total angular momentum of the non-relativistic charge-monopole system with the replacement of the monopole charge g to a matrix value, $g - \frac{1}{2}\sigma_z$. The Dirac operator is a singlet under the $SU(2)$ transformation generated by J_i ,

$$[J_i, -i\mathcal{D}] = 0, \quad (2.12)$$

and so there exist the simultaneous eigenstates (2.7) of the Dirac operator and the $SU(2)$ Casimir. Each relativistic Landau level accommodates the $SU(2)$ degeneracy (2.6), $2j+1 = 2(g+n)$.

The Dirac operator also respects the chiral symmetry,

$$\{-i\mathcal{D}, \sigma_z\} = 0, \quad (2.13)$$

and the spectrum of the Dirac operator is symmetric with respect to the zero eigenvalue (2.5). The non-zero Landau level eigenstates of same eigenvalue magnitude (2.7a) are related by the chiral transformation:

$$\psi_{\pm\lambda_n, m}^g = \sigma_z \psi_{\mp\lambda_n, m}^g. \quad (2.14)$$

A. Mass deformation

We consider a mass deformation to the Dirac operator:

$$-i\mathcal{D} + \sigma_z M = \frac{1}{R_s} \begin{pmatrix} R_s M & -i\mathfrak{D}_-^{(g+\frac{1}{2})} \\ -i\mathfrak{D}_+^{(g-\frac{1}{2})} & -R_s M \end{pmatrix}. \quad (2.15)$$

The mass deformation does not break the $SU(2)$ rotational symmetry of the system

$$[\sigma_z M, J_i] = 0, \quad (2.16)$$

but break the chiral symmetry, $\{\sigma_z M, \sigma_z\} = 2M \neq 0$. The square of the mass deformed Dirac operator yields

$$(-i\not{D} + \sigma_z M)^2 = (-i\not{D})^2 + M^2, \quad (2.17)$$

and the eigenvalues of the mass deformed Dirac operator are obtained as

$$n = 1, 2, \dots : \pm \Lambda_n = \pm \frac{1}{R_s} \sqrt{n(n+2g) + (MR_s)^2}, \quad (2.18a)$$

$$n = 0 : \Lambda_0 = +M. \quad (2.18b)$$

Note that for $n \geq 1$ the spectra (2.18a) still respect the reflection symmetry with respect to the zero energy, while $n = 0$ (2.18b) does not have its counterpart with the negative energy $-M$ [Fig.2]. This asymmetry is a manifestation of the ‘‘parity anomaly’’. The corresponding eigenstates for (2.18) are respectively given by

$$n = 1, 2, \dots :$$

$$\psi_{\pm \Lambda_n, m}^g = \frac{1}{\sqrt{2\Lambda_n(\Lambda_n \mp \lambda_n)}} (\pm M \psi_{\lambda_n, m}^g + (\Lambda_n \mp \lambda_n) \psi_{-\lambda_n, m}^g), \quad (2.19a)$$

$$n = 0 : \psi_{\Lambda_0=M, m}^g = \psi_{\lambda_0=0, m}^g, \quad (2.19b)$$

where $m = -n - g + \frac{1}{2}, -n - g + \frac{3}{2}, \dots, n + g - \frac{1}{2}$. One may find that $\psi_{\Lambda_0=M, m}^g$ (2.19b) is the zero-modes of the massless Dirac operator themselves, while $\psi_{+\Lambda_n, m}^g$ and $\psi_{-\Lambda_n, m}^g$ (2.19a) are linear combinations of the chirality partners of non-zero Landau levels, $\psi_{+\lambda_n, m}^g$ and $\psi_{-\lambda_n, m}^g$, and reduced to them in $M \rightarrow 0$. The mass deformation is inert to the Landau level degeneracy; each of the Landau levels $\pm \Lambda_n$ has the same degeneracy $d_{\pm \Lambda_n} = 2(g+n)$, since the $SU(2)$ symmetry is kept exact even under the mass deformation.

Meanwhile in $M \rightarrow \infty$ which we call the non-relativistic limit, the positive Landau level spectra (2.18a) are reduced to

$$+ \Lambda_n \simeq M + \frac{1}{2MR_s^2} n(n+2g) + O\left(\frac{1}{M^3}\right), \quad (2.20)$$

and the eigenstates (2.19a) are

$$\psi_{+\Lambda_n, m}^g \simeq \frac{1}{\sqrt{2}} (\psi_{\lambda_n, m}^g + \psi_{-\lambda_n, m}^g) = \begin{pmatrix} Y_{j=g-\frac{1}{2}+n, m}^{g-\frac{1}{2}} \\ 0 \end{pmatrix}. \quad (2.21)$$

Notice that the next leading order term on the right-hand side of (2.20) is equal to the non-relativistic Landau levels [17]:

$$E_n = \frac{1}{2MR_s^2} (n(n+2g+1) + g), \quad (2.22)$$

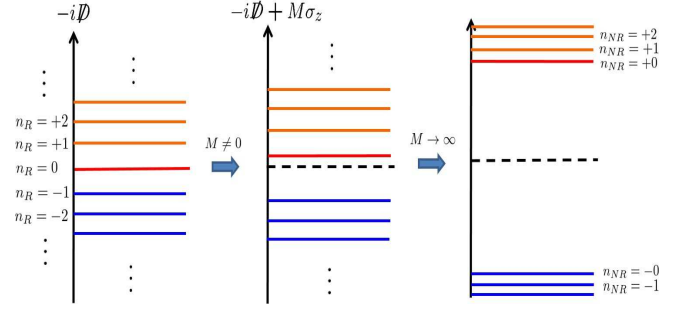


FIG. 2. (Color online) The change of the Dirac operator spectrum under the mass deformation. n_R corresponds to the relativistic Landau level by $\text{sgn}(n_R) \cdot \Lambda_{n=|n_R|}$, and n_{NR} to the non-relativistic Landau level by $\text{sgn}(n_{NR}) \cdot E_{n=|n_{NR}|}$. The mass deformation brings the asymmetry of the spectrum due to the presence of $n_R = 0$ Landau level $\Lambda_{n=0} = +M$ (the red line in the middle figure). In the non-relativistic limit (the right figure), the spectrum yields the non-relativistic Landau level spectrum. Notice that each of the negative relativistic Landau levels decreases (the absolute value of) its Landau level index by one in the non-relativistic Landau level as $|n_{NR}| = |n_R| - 1$.

with replacement from (n, g) to $(n, g - \frac{1}{2})$ up to a unimportant constant and for the eigenstates (2.21) also. Thus in the non-relativistic limit, n th positive relativistic Landau level is reduced to n th non-relativistic Landau level with monopole charge $g - \frac{1}{2}$. Similarly for the negative relativistic Landau level, we have

$$- \Lambda_n \simeq -M - \frac{1}{2MR_s^2} n(n+2g) + O\left(\frac{1}{M^3}\right), \quad (2.23)$$

and

$$\psi_{-\Lambda_n, m}^g \simeq \frac{1}{\sqrt{2}} (-\psi_{\lambda_n, m}^g + \psi_{-\lambda_n, m}^g) = i \begin{pmatrix} 0 \\ Y_{j=g+\frac{1}{2}+(n-1), m}^{g+\frac{1}{2}} \end{pmatrix}. \quad (2.24)$$

The next leading order term of the opposite sign on the right-hand side of (2.23) is equal to the non-relativistic Landau level (2.22) with replacement from (n, g) to $(n-1, g + \frac{1}{2})$ and for the eigenstates (2.24) also. Thus in the non-relativistic limit, up to a constant, (the absolute value of) the n th negative relativistic Landau level reproduces $(n-1)$ th non-relativistic Landau level with monopole charge $g + \frac{1}{2}$.

To summarize, the mass parameter interpolates the n th positive/negative relativistic Landau level physics ($M \rightarrow 0$) and the $n/n-1$ non-relativistic Landau physics ($M \rightarrow \infty$). It is important to note that the positive and negative relativistic Landau levels approach to the different non-relativistic Landau levels in the $M \rightarrow \infty$ limit. We will revisit this in the context of many-body physics in Sec.IV.

III. RELATIVISTIC PSEUDOPOTENTIAL

We next construct a relativistic pseudopotential on the Haldane sphere. Neglecting Landau level mixing, the projection Hamiltonian onto the n th Landau level is given by

$$H = \sum_{p < q} \sum_J V_J^n P_{p,q}(J) \quad (3.1)$$

where V_J^n is Haldane's pseudopotential in n th Landau level and $P_{p,q}(J)$ projects onto states in which p th and q th particles have two-body angular momentum J . $P_{p,q}(J)$ is given by

$$P_{p,q}(J) = \prod_{J' \neq J} \frac{(\mathbf{J}_p + \mathbf{J}_q)^2 - J'(J' + 1)}{J(J + 1) - J'(J' + 1)} \quad (3.2)$$

where \mathbf{J}_p (2.10) represents the angular momentum operator for the p th particle and $J(J + 1)$ is the eigenvalue of $(\mathbf{J}_p + \mathbf{J}_q)^2$. Due to the Wigner-Eckart theorem, the pseudopotential can be expressed as

$$V_J^n \delta_{J_z, J'_z} = \langle\langle J, J_z | V | J, J'_z \rangle\rangle \quad (3.3)$$

where V is Coulomb interaction and $|J, J_z\rangle$ and J_z respectively denote a two-particle state and azimuthal angular momentum.

Let us begin with the massless case. For notational brevity, we rewrite the relativistic eigenstates (2.7a) as the state vector $|j, m, g\rangle$:

$$|j, m, g\rangle_{\pm\lambda_n} = \frac{1}{\sqrt{2}} (|j, m, g - \frac{1}{2}\rangle |\uparrow\rangle \mp i |j, m, g + \frac{1}{2}\rangle |\downarrow\rangle) \quad (3.4)$$

where

$$\langle\theta, \phi | j, m, g \pm \frac{1}{2} \rangle = Y_{j,m}^{g \pm \frac{1}{2}}(\theta, \phi),$$

$$|\uparrow\rangle = \begin{pmatrix} 1 \\ 0 \end{pmatrix}, \quad |\downarrow\rangle = \begin{pmatrix} 0 \\ 1 \end{pmatrix}.$$

The two-particle state $|J, J_z\rangle$ is defined by

$$|J, J_z\rangle_{\pm\lambda_n} = \sum_{m_1, m_2} C_{jm_1, jm_2}^{J, J_z} |j, m_1, g\rangle_{\pm\lambda_n} \otimes |j, m_2, g\rangle_{\pm\lambda_n} \quad (3.5)$$

where $C_{jm, jm'}^{J, J_z}$ represents Clebsch-Gordan coefficients:

$$C_{jm, jm'}^{J, J_z} = (-1)^{J_z} \sqrt{2J + 1} \begin{pmatrix} j & j & J \\ m & m' & -J_z \end{pmatrix}, \quad (3.6)$$

where (\dots) denotes the $3j$ -symbol. Substituting Eq. (3.4) to Eq. (3.5), we have

$$\begin{aligned} |J, J_z\rangle_{\pm\lambda_n} = & \frac{1}{2} \sum_{m_1, m_2} C_{jm_1, jm_2}^{J, J_z} \\ & \times [|j, m_1, g - \frac{1}{2}; j, m_2, g - \frac{1}{2}\rangle |\uparrow, \uparrow\rangle \\ & \mp i |j, m_1, g - \frac{1}{2}; j, m_2, g + \frac{1}{2}\rangle |\uparrow, \downarrow\rangle \\ & \mp i |j, m_1, g + \frac{1}{2}; j, m_2, g - \frac{1}{2}\rangle |\downarrow, \uparrow\rangle \\ & - |j, m_1, g + \frac{1}{2}; j, m_2, g + \frac{1}{2}\rangle |\downarrow, \downarrow\rangle]. \end{aligned} \quad (3.7)$$

With (3.7), the relativistic pseudopotential (3.3) is evaluated as

$$V_J^R = \frac{1}{4} \sum_{\alpha, \beta = g \pm \frac{1}{2}} V_J(j, \alpha, \beta) \quad (3.8)$$

where

$$\begin{aligned} V_J(j, \alpha, \beta) = & (2j + 1)^2 (-1)^{\alpha + \beta} \frac{1}{R_s} \sum_{m_1, m_2, n_1, n_2} C_{jm_1, jm_2}^{J, J_z} C_{jn_1, jn_2}^{J, J_z} \sum_{k=0}^{2j} \begin{pmatrix} j & k & j \\ -\alpha & 0 & \alpha \end{pmatrix} \begin{pmatrix} j & k & j \\ -\beta & 0 & \beta \end{pmatrix} \\ & \times (-1)^{m_1 + m_2} \sum_{m'=-k}^k (-1)^{m'} \begin{pmatrix} j & k & j \\ -m_1 & -m' & n_1 \end{pmatrix} \begin{pmatrix} j & k & j \\ -m_2 & m' & n_2 \end{pmatrix}. \end{aligned} \quad (3.9)$$

Notice that the relativistic pseudopotential (3.8) is the average of the four pseudopotentials $V_J(j, \alpha, \beta)$ with $(\alpha, \beta) = (g - \frac{1}{2}, g - \frac{1}{2}), (g + \frac{1}{2}, g + \frac{1}{2}), (g - \frac{1}{2}, g + \frac{1}{2})$ and $(g + \frac{1}{2}, g - \frac{1}{2})$. The first two correspond to the pseudopotentials of n and $n - 1$ non-relativistic Landau levels respectively. (Remember $j = g - \frac{1}{2} + n = g + \frac{1}{2} + (n - 1)$.) The remaining two come from the cross term between n th and $(n - 1)$ th non-relativistic Landau levels, which are unique pseudopotentials in the relativistic case.

Next we move to the massive case. The relativistic eigenstate (2.19a) can be rewritten as

$$\begin{aligned} |j, m, g, M\rangle_{\pm\lambda_n} = & \frac{1}{2\sqrt{\Lambda(\Lambda_n \mp \lambda_n)}} \\ & \times [(\pm M + \Lambda_n \mp \lambda_n) |j, m, g - \frac{1}{2}\rangle |\uparrow\rangle \\ & + i (\mp M + \Lambda_n \mp \lambda_n) |j, m, g + \frac{1}{2}\rangle |\downarrow\rangle], \end{aligned} \quad (3.10)$$

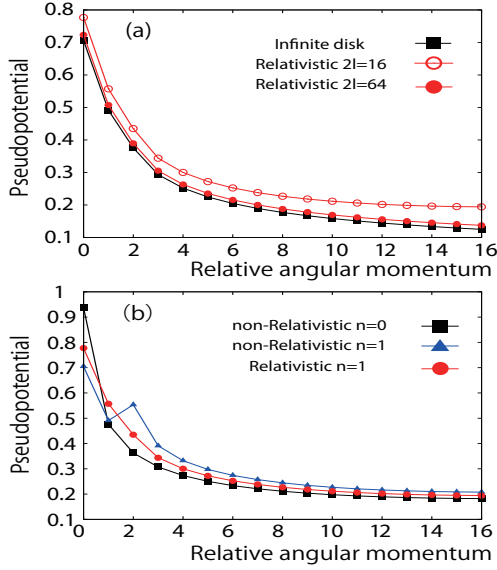


FIG. 3. (Color online) (a) Total flux dependence of the pseudopotential for the relativistic massless particles (3.8) in $n = 1$. The open and filled circles show V_m^R with $N_\Phi = 16$ and 64 , respectively. The solid squares represent the pseudopotential with $N_\Phi = 16$ for the infinite disk geometry. (b) pseudopotential in the various cases. The filled squares and triangles exhibit V_m^{nR} in $n = 0$ and $n = 1$. The solid circles show the relativistic pseudopotential in $n = 1$.

and in a similar manner to the massless case, the pseudopotentials are derived as

$$V_J^R(M)_{\pm\Lambda_n} = \frac{1}{16\Lambda_n^2(\Lambda_n \mp \lambda_n)^2} \quad (3.11)$$

$$\times \left[(\pm M + \Lambda_n \mp \lambda_n)^4 V_J(j, g - \frac{1}{2}, g - \frac{1}{2}) \right. \\ + \{(-M^2 + (\Lambda_n \mp \lambda_n)^2)\}^2 V_J(j, g - \frac{1}{2}, g + \frac{1}{2}) \\ + \{(-M^2 + (\Lambda_n \mp \lambda_n)^2)\}^2 V_J(j, g + \frac{1}{2}, g - \frac{1}{2}) \\ \left. + (\mp M + \Lambda_n \mp \lambda_n)^4 V_J(j, g + \frac{1}{2}, g + \frac{1}{2}) \right].$$

Since the $SU(2)$ generators are immune to the mass deformation, the mass deformation affects the projection Hamiltonian (3.1) only through the pseudopotentials (3.11).

In the following discussions, we express the pseudopotentials as a function of the relative angular momentum $m = 2j - J$.

IV. NUMERICAL RESULTS

To investigate physics of the mass deformation on many-body states, we perform exact diagonalization study at $\nu = \frac{1}{3}$ in this section. We focus on single Dirac Hamiltonian, which describes surface electron of 3D topological insulator or graphene with fully polarized spin and

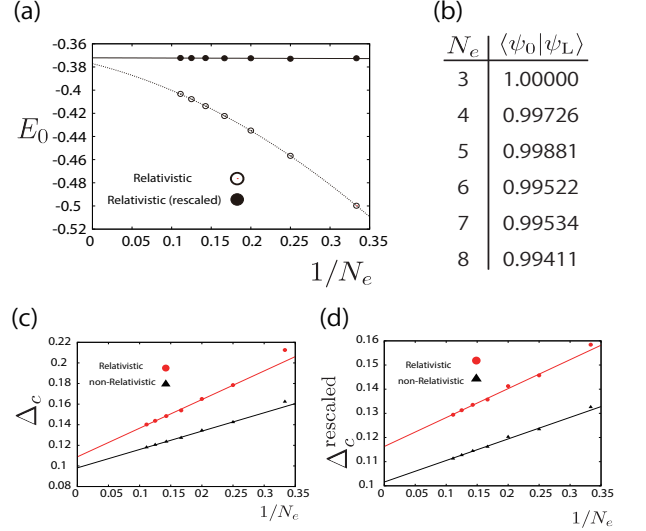


FIG. 4. (Color online) (a) Ground state energies as a function $1/N_e$. The open and filled circles represent the lowest energies in unit of $e^2/\epsilon l_B$ and $e^2/\epsilon l'_B$, respectively. The solid (dotted) line shows the linear (square) fitting for each of the energies. (b) Overlaps for each N_e . (c) and (d) show the charge gap and the rescaled one, respectively. The circles (triangles) represent the relativistic (non-relativistic) results.

valley degrees of freedom. In the following, we set $e^2/\epsilon l_B$ to unity. (ϵ is a dielectric constant.) It is well known that the ground state is described by Laughlin state at $\nu = \frac{1}{q}$ (q is odd integer) [25]. In the spherical geometry, Laughlin state realizes when the total flux N_Φ is given by [17, 26]

$$N_\Phi = 2j = \nu^{-1}(N_e - 1) \quad (4.1)$$

where N_e is the number of electrons. We define the total energy as

$$E(N_\Phi) = E_C(N_\Phi) - \frac{N_e^2}{2R_s} \quad (4.2)$$

where the first term represents the energy of Coulomb interaction and the second term means the effect of the neutralizing background and the self-energy of the background.

We also assess energy gap for the creation of quasiparticle or quasihole as

$$\Delta_c^\pm = E(N_\Phi \pm 1) - E(N_\Phi) \quad (4.3)$$

where $+/-$ corresponds to quasihole/quasiparticle. These excitation gap within a system in the thermodynamic limit is given by $\Delta_c = \Delta_c^+ + \Delta_c^-$.

A. Massless case

We investigate the massless relativistic case for comparison to the non-relativistic results obtained by Fano

et al [27]. We demonstrate the numerical results only for $+\lambda_n$ because the pseudo-potential Hamiltonian for $+\lambda_n$ is equivalent to that for $-\lambda_n$. Fig. 3 (a) shows the total flux dependence of the relativistic pseudopotential V_m^R in $n = 1$. In Fig. 3 (a), we also show the pseudopotential in infinite disk geometry [28]

$$V_m^{\text{Disk}} = \int \frac{dq}{2\pi} q V(q) [F_n(q)]^2 L_m(q^2) e^{-q^2}. \quad (4.4)$$

Here $F_n(q)$ is the relativistic form factor [29]

$$F_n(q) = \frac{1}{2} [L_n(q^2/2) + L_{n-1}(q^2/2)] \quad (4.5)$$

where $L_n(x)$ represents Laguerre polynomials.

It is expected that V_m^R and V_m^{Disk} become equivalent in the thermodynamic limit $N_\Phi \rightarrow \infty$ because the finite size effect of the sphere will vanish in $R_s = \sqrt{g} l_B \rightarrow \infty$. (l_B is the magnetic length, $l_B = \sqrt{c\hbar/eB}$.) Indeed, with the increase of the total flux l , V_m^R apparently approach to V_m^{Disk} in Fig.3 (a). Thus we confirm the equivalence between the disc and spherical geometries in the thermodynamic limit.

In Fig. 3(b) we compare m -dependence of the pseudopotentials between the relativistic V_m^R in $n = 1$ and the non-relativistic $V_m^{\text{NR}} (= V_J(j, g, g)|_{j=n+g})$ in $n = 0$ and 1. Since the stability of Laughlin state at $\nu = \frac{1}{3}$ strongly depends on $V_1 - V_3$ [26], we focus on $V_1 - V_3$ in Fig.3(b). The value of $V_1 - V_3$ of $n = 1$ non-relativistic Landau level is the smallest, and hence its Laughlin state is considered to be unstable. (Also notice that the pseudopotential shows a cusp at the relative angular momentum $m = 2$.) Meanwhile, the $n = 1$ relativistic pseudopotential V_m^R shows a monotonic decay as a function of the relative angular momentum and its $V_{m=1}^R - V_{m=3}^R$ is the largest. Therefore, the Laughlin state in the $n = 1$ relativistic level is expected to be more stable than those of the non-relativistic levels $n = 0, 1$ [18, 21].

The open circles in Fig. 4(a) show the lowest energies for each N_e and the filled circles in Fig. 4(a) show the lowest energies rescaled by $l'_B = (N_\Phi \nu / N_e)^{1/2} l_B$. The energies in the unit of $e^2/\epsilon l'_B$ give us good extrapolated values even if the number of electrons are small [30]. The filled circles behave as a linear function to have $E_0(N_\Phi \rightarrow \infty) \approx -0.3721$.

Fig. 4(b) exhibits the overlaps $\langle \psi_0 | \psi_L \rangle$ between the numerical ground state $|\psi_0\rangle$ and the Laughlin wave function $|\psi_L\rangle$. The Laughlin state has a remarkably large overlap $\langle \psi_0 | \psi_L \rangle$ for each N_e more than 99%, which strongly suggests that the many-body groundstate of the $n = 1$ relativistic Landau level is the Laughlin state.

Fig. 4(c) displays the charge gap Δ_c for the $n = 1$ relativistic and non-relativistic Landau levels, and Fig. 4(d) exhibits the rescaled charge gap $\Delta_c^{\text{rescaled}}$. The charge gap in the relativistic Landau level is larger than that in the non-relativistic level. This is expected from the previous observation that the Laughlin state in the relativistic Landau level is more stable than in the non-relativistic

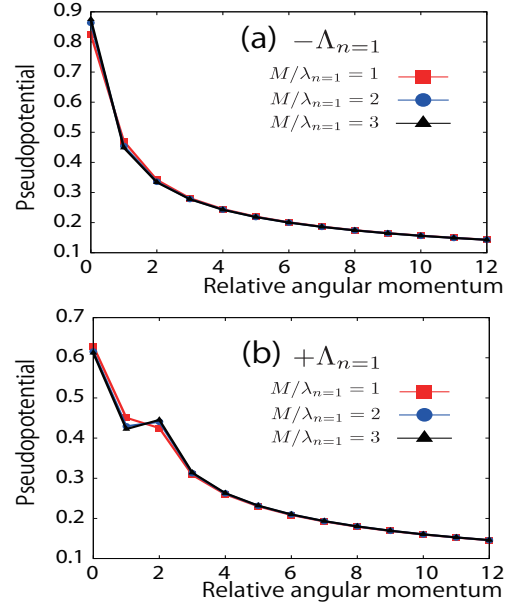


FIG. 5. (Color online) Mass dependence of the pseudopotential with $N_\Phi = 12$. (a) and (b) show the numerical results in $+\Lambda_{n=1}$ and $-\Lambda_{n=1}$, respectively.

Landau level. From the rescaled charge gap, we obtain $\Delta_c \approx 0.1163$. This value is in agreement with previous work using V_m^{Disk} in larger systems [18].

B. Massive case

We investigate the mass effect on the $n = 1$ positive and negative relativistic Landau levels. We focus on Laughlin state of $n = 1$ since it is stable in the massless limit. Fig. 5(a) and (b) show mass dependence of the pseudopotentials. As shown in Fig. 5(a), for the negative relativistic Landau level $-\Lambda_{n=1} < 0$, V_m^R slightly decrease with increase of $M/\lambda_{n=1}$ and monotonically decrease for the relative momentum m as in the massless case. For the positive Landau level $+\Lambda_{n=1}$, the pseudopotential shows an intriguing behavior: In small $M/\lambda_{n=1}$, its behavior is similar to that of the massless case in Fig.3(a), while with the increase of $M/\lambda_{n=1}$, the pseudopotential shows a cusp at $m = 2$ which is the unique feature of the $n = 1$ non-relativistic pseudopotential as shown in Fig.3(b). Thus also for the many-body state, the mass parameter is expected to interpolate the relativistic physics ($M \rightarrow 0$) and non-relativistic one ($M \rightarrow \infty$).

The overlap $\langle \psi_0 | \psi_L \rangle$ in $N_e = 7, 8$ and 9 system as a function of $M/\lambda_{n=1}$ is shown in Fig. 6(a). The overlap in the negative relativistic Landau level $-\Lambda_{n=1}$ keeps large values more than 99% all over $M/\lambda_{n=1}$ (left-figure). Meanwhile, the overlap in the relativistic positive Landau level $+\Lambda_{n=1}$ rapidly decreases with increasing $M/\lambda_{n=1}$ (right-figure) and finally reduces to about 50% in $N_e = 9$ system in large $M/\lambda_{n=1}$ region. The rescaled charge gap

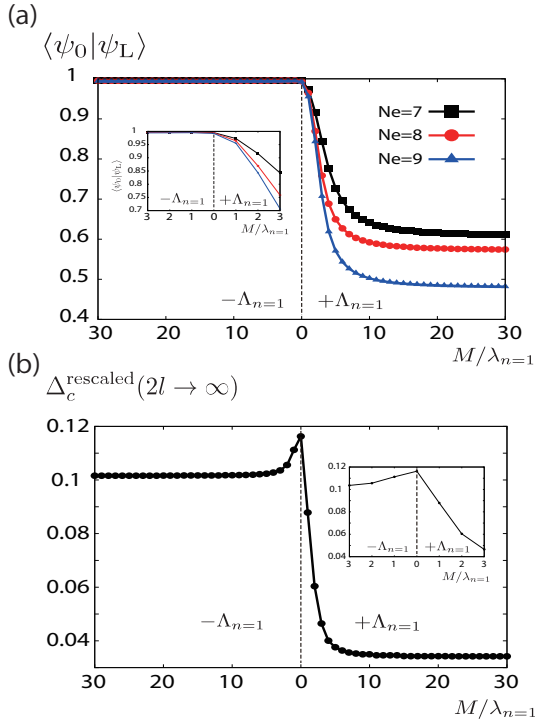


FIG. 6. (Color online) (a) Mass dependence of the overlaps between the numerical ground state and Laughlin wave function in $N_e = 7, 8$ and 9 system. (b) Charge gap in thermodynamic limit with unit of $e^2/\epsilon l'_B$. Insets in (a) and (b) show the numerical results in $0 \leq M/\lambda_{n=1} \leq 3$

$\Delta_c^{\text{rescaled}}$ in thermodynamic limit $N_\Phi \rightarrow \infty$ also shows a rapid decay in $+\Lambda_{n=1}$ as shown in Fig. 6(b). Thus the Laughlin state is no longer a good candidate for the ground state with large $M/\lambda_{n=1}$ in $+\Lambda_n$.

Let us consider these results in view of the parity anomaly. In the massless case, the relativistic system respects the chiral symmetry and so the pseudopotentials in the positive and negative relativistic Landau levels are equivalent. When M is turned on, accompanied with the chiral symmetry breaking, the mass deformed pseudopotentials in $\pm\Lambda_n$ begin to split according to (3.11). Since in the non-relativistic limit ($M \rightarrow \infty$), $\psi_{+\Lambda_n}$ and $\psi_{-\Lambda_n}$ are reduced to the non-relativistic eigenstates in n th and $(n-1)$ th Landau levels [remember the discussions in Sect. II A], $V_J^R(M)_{+\Lambda_n}$ and $V_J^R(M)_{-\Lambda_n}$ are also reduced to the non-relativistic pseudopotentials of the n and $(n-1)$ th Landau levels respectively. As a result, while the ground state in $-\Lambda_{n=1}$ keeps being characterized by the Laughlin state, the Laughlin state in $+\Lambda_{n=1}$ become unstable in large M region. Thus, the “parity anomaly” brings inequivalence also to the many-body physics of the relativistic quantum Hall effect.

V. SUMMARY AND DISCUSSIONS

We constructed an exact form of the relativistic pseudopotentials and demonstrated numerical calculations of the relativistic quantum Hall liquid on the Haldane sphere. Specifically, we analyzed the properties of the relativistic quantum Hall liquid at $\nu = \frac{1}{3}$ by the exact diagonalization. Though in the massless case either of relativistic many-body groundstates for the $n = 1$ positive and negative relativistic Landau levels are well described by the Laughlin wavefunction, our numerical results strongly suggest that the mass term brings instability to the Laughlin state of the positive relativistic Landau level $n = 1$ and the Laughlin state no longer well describes the many-body groundstate in the presence of a sufficiently large mass.

Here we note the energy scale of the mass term in experimental Dirac matter. For graphene and topological insulator (Bi_2Se_3) [31, 32], the relativistic Landau level spacing $\sqrt{2}\hbar v_F/l_B \approx 4v_F\sqrt{B[\text{T}]} \times 10^{-5}$ meV (v_F means Fermi velocity) is estimated to be the order of 1×10^6 and 1×10^5 m/s respectively. Meanwhile, for mass gap, Zhou *et al* reported the energy gap by the breaking of AB sublattice symmetry of graphene as 260 meV [11], and Chen *et al* estimated the gap size of topological insulator surface of Bi_2Se_3 with 16% Fe doping about 50 meV [13]. Thus for both graphene and topological insulator surface, the mass parameter is comparable with (or even larger than) the Landau level spacing with controlling external magnetic field. Therefore, it is expected that the present results will be observable in real Dirac matter.

ACKNOWLEDGMENTS

KH would like to thank Hiroaki Matsueda for arranging a seminar at Tohoku University which enabled the present collaboration. This work was supported by Grants-in-Aid for Scientific Research (No. 26400344) from MEXT Japan.

Appendix A: Derivation of the pseudopotential

We derive the explicit representation of V_J^R (3.8) using the method of Ref.[33]. From the definition of the pseudopotential and two-particle state, $V(j, \alpha, \beta)$ in the main text are given by

$$V(j, \alpha, \beta) = \sum_{m_1, m_2, n_1, n_2} C_{jm_1, jm_2}^{J, J_z} C_{jn_1, jn_2}^{J, J_z} \langle j, m_1, \alpha; j, m_2, \beta | V | j, n_1, \alpha; j, n_2, \beta \rangle. \quad (\text{A.1})$$

Here, V is the Coulomb interaction on the sphere which can be expressed as

$$V(r_1 - r_2) = \frac{e^2}{\epsilon R_s} \sum_{k=0}^{\infty} \frac{4\pi}{2k+1} \sum_{m'=-k}^k Y_{k,m'}(\Omega_1)^* Y_{k,m'}(\Omega_2) \quad (\text{A.2})$$

where $Y_{k,m'}$ is a spherical harmonics and Ω_p means the spherical coordinate (θ_p, ϕ_p) for the p th particle. The matrix elements of (A.1) are written as

$$\begin{aligned} \langle j, m_1, \alpha; j, m_2, \beta | V | j, n_1, \alpha; j, n_2, \beta \rangle = \\ \frac{e^2}{\epsilon R_s} \sum_{k=0}^{\infty} \sum_{m'=-k}^k \frac{4\pi}{2k+1} \\ \times \int Y_{j,m_1}^{\alpha}(\Omega_1)^* Y_{k,m'}(\Omega_1)^* Y_{j,n_1}^{\alpha}(\Omega_1) d\Omega_1 \\ \times \int Y_{j,m_2}^{\beta}(\Omega_2)^* Y_{k,m'}(\Omega_2) Y_{j,n_2}^{\beta}(\Omega_2) d\Omega_2. \end{aligned} \quad (\text{A.3})$$

Using properties of the monopole harmonics [22, 23]

$$Y_{k,m'}(\Omega) = Y_{k,m'}^0(\Omega) \quad (\text{A.4a})$$

$$Y_{j,m}^Q(\Omega)^* = (-1)^{Q+M} Y_{j,-m}^{-Q}(\Omega) \quad (\text{A.4b})$$

$$\begin{aligned} \int Y_{j,m}^Q(\Omega) Y_{k,m}^0(\Omega) Y_{j,n}^Q(\Omega) d\Omega = (-1)^{2j+k} \times \\ \left[\frac{(2j+1)(2k+1)(2j'+1)}{4\pi} \right]^{1/2} \begin{pmatrix} j & k & j \\ -Q & 0 & Q \end{pmatrix} \begin{pmatrix} j & k & j \\ m & m' & n \end{pmatrix}, \end{aligned} \quad (\text{A.4c})$$

we can represent (A.3) as

$$\begin{aligned} \langle j, m_1, \alpha; j, m_2, \beta | V | j, n_1, \alpha; j, n_2, \beta \rangle = \\ \frac{e^2}{\epsilon R_s} \sum_{k=0}^{2j} \sum_{m'=-k}^k (2j+1)^2 \begin{pmatrix} j & k & j \\ -\alpha & 0 & \alpha \end{pmatrix} \begin{pmatrix} j & k & j \\ -\beta & 0 & \beta \end{pmatrix} \\ \times \begin{pmatrix} j & k & j \\ -m_1 & -m' & n_1 \end{pmatrix} \begin{pmatrix} j & k & j \\ -m_2 & m' & n_2 \end{pmatrix}. \end{aligned} \quad (\text{A.5})$$

We note that $\sum_{k=0}^{\infty}$ reduces a finite sum up to $2j$ since $3j$ -symbol is finite for $0 \leq k \leq 2j$.

-
- [1] P. R. Wallace, Phys. Rev. **71**, 622 (1947).
 - [2] S. Y. Zhou, G. -H. Gweon, J. Graf, A. V. Fedorov, C. D. Spataru, R. D. Diehl, Y. Kopelevich, D. -H. Lee, Steven. G. Louie, and A. Lanzara, Nature physics **2**, 595 (2006).
 - [3] Aaron Bostwick, Taisuke Ohta, Thomas Seyller, Karsten Horn, and Eli Rotenberg, Nature physics **3**, 36 (2007).
 - [4] Haijun Zhang, Chao-Xing Liu, Xioa-Liang Qi, Xi Dai, Zhong Fang, and Shou-Cheng Zhang, Nature physics **5**, 438 (2009).
 - [5] Yuanbo Zhang, Yan-Wen Tan, Horst L. Stormer, and Philip Kim, Nature **438**, 201 (2005).
 - [6] K. S. Novoselov, A. K. Geim, S. V. Morozov, D. Jiang, M. I. Katsnelson, I. V. Grigorieva, S. V. Dubonos, and A. A. Firsov, Nature **438**, 197 (2005).
 - [7] Kirill I. Bolotin, Fereshte Ghahari, Michael D. Shulman, Horst L. Stormer, and Philip Kim, Nature Phys. **462**, 196 (2009).
 - [8] R. Yoshimi, A. Tsukazaki, Y. Kozuka, J. Falson, K. S. Takahashi, J. G. Checkelsky, N. Nagaosa, M. Kawasaki, and Y. Tokura, Nature communications **6**, 6627 (2015).
 - [9] Yang Xu, Ireneusz Miotkowski, Chang Liu, Jifa Tian, Hyoungdo Nam, Nasser Alidoust, Jiuning Hu, Chih-Kang Shih, M. Zahid Hasan, and Yong P. Chen, Nature Physics **10**, 956 (2014).
 - [10] X.-L. Qi, T.L. Hughes, and S.-C. Zhang, Phys. Rev. B **78**, 195424 (2008).
 - [11] S. Y. Zhou, G. -H. Gweon, A. V. Fedorov, P. N. First, W. A. de Heer, D. -H. Lee, F. Guinea, A. H. Castro Neto, and A. Lanzara, Nature Materials **6**, 770 (2007).
 - [12] V. M. Pereira, J. M. B. Lopes dos Santos, and A. H. Castro Neto, Phys. Rev. B **77**, 115109 (2008).
 - [13] Y. L. Chen, J. -H. Chu, J. G. Analytis, X. K. Liu, K. Igarashi, H. -H. Kuo, X. L. Qi, S. K. Mo, R. G. Moore, D. H. Lu, M. Hashimoto, T. Sasagawa, S. C. Zhang, I. R. Fisher, X. Hussain, and Z. X. Shen, Science **329**, 659 (2010).
 - [14] The parity anomaly is usually referred to as the parity breaking Chern-Simons term induced by quantum effect. In the present paper the ‘‘parity anomaly’’ is referred to as asymmetry of the positive and negative Landau levels due to the (parity breaking) mass term in (2+1)D.
 - [15] The mass term does not necessarily violate the reflection symmetry of the Dirac operator spectrum with respect to the zero energy. For instance in the case of the free Dirac operator, the mass deformation breaks the chiral symmetry, but the spectrum still preserves the reflection symmetry. The chiral symmetry is a sufficient condition of the reflection symmetry of the spectrum but not a necessary condition.
 - [16] F. D. M. Haldane, Phys. Rev. Lett. **61**, 2015 (1988).
 - [17] F. D. M. Haldane, Phys. Rev. Lett. **51**, 605 (1983).
 - [18] Naokazu Shibata and Kentaro Nomura, J. Phys. Soc. Jpn. **78**, 104708 (2009).
 - [19] K. Hasebe, arXiv:1511.04681.
 - [20] C. Töke, P. E. Lammert, V. H. Crespi, and J. K. Jain, Phys. Rev. B **74**, 235417 (2006).
 - [21] V. M. Apalkov and T. Chakraborty, Phys. Rev. Lett. **97**, 126801 (2006).
 - [22] Tai Tsun Wu and Chen Ning Yang, Nucl. Phys. B **107**, 365 (1976).
 - [23] Tai Tsun Wu and Chen Ning Yang, Phys. Rev. D **16**, 1018 (1977).
 - [24] E. T. Newman and R. Penrose, J. Math. Phys. **7**, 863 (1966).
 - [25] R. B. Laughlin, Phys. Rev. Lett. **50**, 1395 (1983).

- [26] F. D. M. Haldane and E. H. Rezayi, Phys. Rev. Lett. **54**, 237 (1985).
- [27] G. Fano, F. Ortolani, and E. Colombo, Phys. Rev. B **34**, 2670 (1986).
- [28] R. E. Prange and S. M. Girvin, *The Quantum Hall Effect* (Springer-Verlag, New York, 1987).
- [29] Kentaro Nomura and Allan H. MacDonald, Phys. Rev. Lett. **96**, 256602 (2006).
- [30] R. H. Morf, N. d’Ambrumenil, and S. Das Sarma, Phys. Rev. B **66**, 075408 (2002).
- [31] S. Das Sarma, Shaffique Adam, E. H. Hwang, and Enrico Rossi, Rev. Mod. Phys. **83**, 407 (2011).
- [32] Peng Cheng, Canli Song, Tong Zhang, Yanyi Zhang, Yilin Wang, Jin-Feng Jia, Jing Wang, Yayu Wang, Bang-Fen Zhu, Xi Chen, Xucun Ma, Ke He, Lili Wang, Xi Dai, Zhong Fang, Xincheng Xie, Xiao-Liang Qi, Chao-Xing Liu, Shou-Cheng Zhang, and Qi-Kun Xue, Phys. Rev. Lett. **105**, 076801 (2010).
- [33] R. E. Wooten and J. H. Macek, arXiv:1408.5379.